Hindawi Publishing Corporation
ISRN Nanotechnology
Volume 2014, Article ID 326747, 8 pages
http://dx.doi.org/10.1155/2014/326747

Research Article

TiO_2 Microwave Synthesis, Electrophoretic Deposition of Thin Film, and Photocatalytic Properties for Methylene Blue and Methyl Red Dyes

A. K. Singh[1] and Umesh T. Nakate[2]

[1] *DRDO Center for Piezoceramics and Devices, ARDE, Pashan, Pune 411007, India*
[2] *Nanomaterials & Sensors Laboratory, Defence Institute of Advanced Technology (DU), Girinagar, Pune 411025, India*

Correspondence should be addressed to A. K. Singh; draksingh@hotmail.com

Received 12 January 2014; Accepted 25 February 2014; Published 7 April 2014

Academic Editors: M. A. Behnajady, M. Fernández-García, and L. Y. Khomenkova

Electrophoretic deposition (EPD) of TiO_2 thin film was carried out at room temperature on low cost steel substrate using microwave synthesized nanoparticles (NPs) of TiO_2. Synthesized NPs and EPD thin film were characterized at different stages of synthesis for its crystal structure, morphology, elemental analysis, and surface area. Spherical particle morphology and formation of TiO_2 were confirmed by scanning electron micrograph (SEM), energy dispersive spectrometer (EDS), and X-ray diffraction (XRD). Synthesized NPs were formed in anatase phase having crystallite size of about 12.3 nm from Scherrer's formula using full width half maxima (FWHM). Surface area was found to be 43.52 m^2/g by BET giving particle size of 33 nm. Photocatalytic (PC) behavior of TiO_2 NPs and EPD TiO_2 film on steel substrate was investigated under UV light for two commercial dyes and their photocatalysis efficiency was analyzed. NPs have shown better efficiency for methylene blue (MB) dye than EPD film whereas EPD film have shown higher PC activity for methyl red (MR) dye.

1. Introduction

TiO_2 is one of the transition metal oxides, having excellent optical, electrical, PC properties [1, 2]. It is optically transparent, nontoxic, wide band gap, and sensitive to UV-radiations. Apart from high photoactivity, TiO_2 is biologically and chemically inert, abundantly available, and cheap. TiO_2, being very reactive with both light and water, exhibits exceptional resistance to corrosion and photocorrosion in aqueous environments. Therefore, TiO_2 in water exhibits stable properties over a prolonged period of time. Other than PC activity, TiO_2 finds applications in the fields of gas sensors, supercapacitors, cosmetics, and solar cells [3, 4]. Because of its strong UV light absorbance, TiO_2 is applied as a sunscreen blocker. The applications of TiO_2 also include self-cleaning coatings, hydrophilic coatings, and antifogging coatings. Under normal atmospheric conditions and UV-Vis light, organisms that are virulent and hard to be decomposed can be thoroughly oxidized to molecules, such as H_2O and CO_2 by using anatase TiO_2 under UV irradiation. PC reaction in the presence of TiO_2 consists of a free radical reaction initiated by absorption of the photon with energy equal to or greater than the band gap of TiO_2. Charge separation, leading to enhanced concentration of electron and holes at the surface, results in a substantial increase of the oxidation power of TiO_2 when immersed in water. Anatase TiO_2 is the most widely explored material for PC applications due to its wide band gap, for example, 3.03 eV for rutile and 3.18 eV for anatase [2]. An enormous research effort has been made to study the PC properties and applications of TiO_2 under light illumination. In particular, for the purification of water from contaminants, TiO_2 is able to photocatalyze many organic substances under UV irradiation. The organic pollutants are serious health problem which are discharged in the environment by industries and houses. Before discharging these harmful organic pollutants these must be degraded or destroyed [5]. In this study an attempt has been made to develop and implement an efficient and cost effective scheme for the purification and disinfection of water from organic dyes.

In literature, several methods such as sol-gel [6], organometallic [7], and hydrothermal [8] have been reported for the synthesis of TiO_2 NPs whereas CVD [9], spray pyrolysis [10], and magnetron sputtering [11] have been used for TiO_2 thin film growth. Microwave synthesis is the novel route of synthesis of TiO_2 NPs which is clean, cost-effective, energy efficient, ecofriendly, rapid, and convenient method of heating and results in higher yields in shorter reaction times [12]. Recently, Pan et al. [13] has reported that microwave synthesized catalysts show improved PC activity compared with one synthesized via traditional methods.

To avoid the use of powder, which is to be separated from the water in a slurry system after PC reaction [14, 15], thin film coating of TiO_2 can be thought of as a good substitute. Baran et al. [16] has proposed thin film coating of TiO_2 and has indicated that thin films can be upgraded to large volume of textile wastes of low concentration. The efficiency may depend on the ability of the degraded compound to be adsorbed on the surface of the catalyst [17]. It is well known that the PC activity of TiO_2 thin films strongly depends on the preparing methods and post-treatment conditions, since they have a decisive influence on the chemical and physical properties of TiO_2 thin films.

EPD is one of the efficient techniques being developed for processing of ceramics, thin film coatings, and composite materials from colloidal suspensions on metallic substrates. Compared with other processing methods, EPD offers advantages of low cost, process simplicity, uniformity of deposition, control of deposit thickness, microstructural homogeneity, and deposition on complex shaped substrates, including the potential to infiltrate porous substrates. EPD allows flexibility to choose conducting substrates of any shape and any size and can be extended to large scale for industrial applications [17]. Low temperature deposition of TiO_2 film using EPD overcomes two main problems such as incomplete necking of the particles and presence of residual organics in the film. These problems lower the diffusion coefficient and decrease the lifetime of the electrons. EPD technique [18] enables the production of unique microstructures and nanostructures as well as complex material combinations in a variety of macroscopic shapes.

There is increasing interest in improving the PC activity of anatase TiO_2. Various techniques such as the methods of improving the crystal phase, morphology, porosity, surface area, loading, and calcinations temperature [19–22]. Optimum degradation has been achieved at PC loading of 0.4–1.5 g/L for different dyes and for calcinations temperatures in the range of 500°C–700°C [23]. In view of the above mentioned and in order to minimize requirement of TiO_2 loading and increase surface area, TiO_2 electrodes had been reported by coating the surfaces of costly electrically conducting substrates such as quartz and indium tin oxide (ITO), with TiO_2 [15, 24, 25]. In the present work, we have synthesized TiO_2 NPs by novel microwave assisted method for EPD of TiO_2. Good quality, porous TiO_2 thin films were deposited on low cost steel substrate. Synthesized NPs and EPD film were investigated for their PC activity using MB and MR dyes after air annealing of samples at 500°C temperature.

2. Materials and Methods

2.1. Materials. Titanium (IV) butoxide reagent grade 97% $Ti[O(CH_2)_3CH_3]_4$ (Sigma-Aldrich), n-butyl alcohol for synthesis $CH_3(CH_2)_3{\cdot}OH$ (LR) (Thomas Baker), deionized (DI) water 18.2 MΩ (Milipore), acetone (LR) (Qualigens fine chemicals), ethyl alcohol AR 99.9% (Changshu Yangyuan Chemicals), iodine LR (Thomas Baker), methylene blue (Aqueous) (Fisher Scientific), and methyl red (HPLC, Mumbai).

2.2. Microwave Synthesis. Above chemicals are used as they are received without any further purification. 0.5 M titanium butoxide solution was prepared in 100 mL butanol and stirred for 15 minutes and further 30 mL deionized water was added drop wise in above solution to allow hydrolysis. This solution was stirred for 30 minutes; this gives rise to white precipitation; this white precipitate microwave irradiated for 5 minutes at 700 W power using RAGA'S microwave. This obtained solution was left 24 hours for aging at room temperature then it is centrifuged at 2000 rpm for 15 minutes. Obtained precipitate was dried at 80°C for 12 hours, after complete drying powder was annealed at 500°C for 2 hours to remove hydroxide impurities and to achieve recrystallization.

2.3. Electrophoretic Deposition (EPD) of TiO_2 Thin Film. The synthesized TiO_2 NPs were used for EPD. EPD was carried out using two-electrode cell where steel substrate was working electrode and graphite was counter electrode. Steel substrate was washed with soap solution, ultrasonicated for 10 minutes in acetone, and again sonicated in DI water for 10 minutes. For EPD deposition electrolyte solution was prepared by adding 0.05 g TiO_2 synthesized NPs in 60 mL acetone. In this solution few drops of iodine were added to increase charging of TiO_2 NPs and sonicated for 10 minutes. The pH of the solution was maintained between 1 and 2 using diluted hydrochloric acid. EPD was carried out at room temperature by keeping distance between two electrodes at 1 cm under application of 30 V. EPD was cathodic since TiO_2 NPs are positively charged. Deposition time was optimized and results presented here for two minutes duration. Subsequently, coated film was rinsed with DI water and dried at room temperature, and finally it was annealed at 500°C in air for 2 hours.

2.4. Characterization. The prepared samples were characterized at different stages of synthesis and EPD. XRD patterns were obtained using Philips XL-30 and Xpert PRO Panalytical Powder XRD in the scanning range of 20–60° (2θ) using Cu Kα radiations with wavelength of 1.54 Å. SEM was performed using JOEL ASM 6360A. Measurement of BET surface area was carried out for nitrogen adsorption using a Micrmeritrics Ins., USA. Optical absorption spectra (UV-Visible) were obtained using Ocean Optics UV-Visible spectrometer in the absorption mode in the wavelength range of 200–1000 nm.

2.5. Photocatalytic (PC) Activity. Microwave synthesized TiO_2 NPs and EPD films deposited on steel (both air annealed)

were used to study photodegradation of MB of high concentration and MR of low concentration in DI water. Photodegradation investigations were carried using 0.005 g TiO_2 NPs and EPD thin film of dimension $1.5 \times 1.5\ cm^2$ in 200 μL/L for MB and 10 mL/L for MR dye solutions. Dye solutions were stirred for 10 minutes in dark for equilibrium of adsorption and desorption process of dye with TiO_2 surface. After stirring, the solution was irradiated by UV lamp (Blue Wave 50 AS, Model 39370 Universal, DYMAX Corporation) medium intensity spot lamp, wavelength range 200–600 nm, and nominal intensity of 1000–2000 mW/cm^2. Concentrations of dye solutions were recorded at the beginning and after irradiation of UV light using Ocean optics UV-Visible spectrometer. From prepared dye solutions of MB and MR, 20 mL and 100 mL solutions were used to analyze photodegradation behavior of EPD TiO_2 film and NPs, respectively, and 5 mL of analytical samples was withdrawn by means of a syringe from the reaction suspensions at predefined times after irradiation. All the PC experiments were performed at room temperature in the dark.

3. Results and Discussion

3.1. Microwave Synthesis. TiO_2 NPs were synthesized by novel microwave assisted method with titanium butoxide as starting material. Titanium butoxide precursor has more reactivity compared to other precursors because of variable oxidation capability. Titanium (IV) butoxide reacts with DI water leading to hydrolysis and condensation. In case of titanium ion precursors, the presence of vacant d orbital can increase the coordination number from 4 to 6. Reaction kinetics is given below:

$$\mathrm{Ti(OCH_4H_9)_4 + 4H_2O = Ti(OH)_4 + 4C_4H_9OH} \quad (1)$$

$$\mathrm{Ti(OH)_4 = TiO_2 \downarrow + 2H_2O} \quad (2)$$

During the precipitation primary particles nucleate initially and these primary particles aggregate to form secondary particles which results in spherical aggregates of nanosized crystalline titania. After microwave irradiation and air annealing, formation of crystalline titanium oxide takes place.

3.2. Electrophoretic Deposition (EPD) of TiO_2 Thin Film. Koura et al. [26] have analyzed the process of EPD using electrification mechanism of an oxide particle in a bath which can be explained using the following equations:

$$\mathrm{CH_3COCH_3 \leftrightarrows CH_3C(OH)CH_2} \quad (3)$$

$$\mathrm{CH_3C(OH)CH_2 + I_2 \longrightarrow CH_3COCH_2I + H^+ + I^-} \quad (4)$$

From (4), it can be understood that acetone releases H^+ions. These ions are adsorbed on TiO_2 NPs and it gets positively charged. Positively charged TiO_2 NPs get attached to cathodic steel electrode. At cathode reduction of H^+ion takes place and TiO_2 particles get deposited on steel substrate.

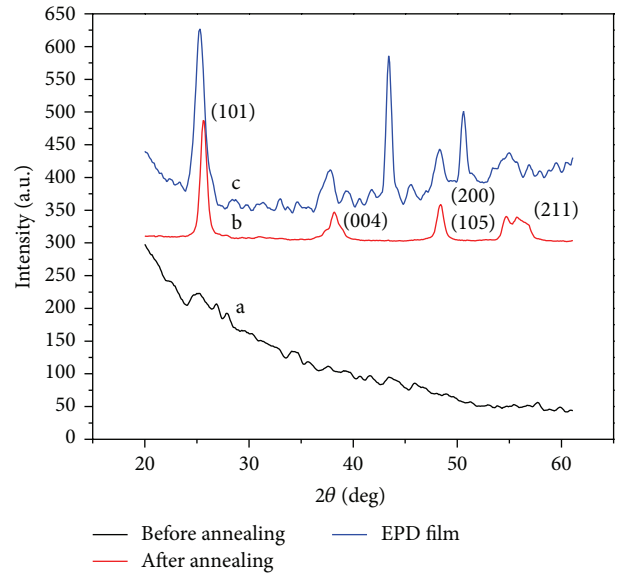

Figure 1: XRD of TiO_2 (a) NPs before annealing, (b) NPs after air annealing at 500°C, and (c) EPD TiO_2 film.

3.3. X-Ray Diffraction (XRD). To confirm the formation of TiO_2, XRD patterns of the TiO_2 NPs, before and after annealing, and of EPD TiO_2 film has been recorded and shown in Figure 1. The diffraction pattern shows that TiO_2 NPs have been crystallized in anatase phase after annealing and highly oriented along (110) plane (JCPDS file 84-1284). The sharpness of peaks shows that TiO_2 NPs are highly crystalline. After EPD additional two peaks at 43.76° and 50.88° have been observed which can be attributed to the steel substrate.

The crystallite size of TiO_2 is calculated using Scherrer's formula [27]:

$$D = \frac{K\lambda}{\beta \mathrm{Cos}\,\theta}, \quad (5)$$

where λ is wavelength of X ray, β is full width and half maxima, and θ is Bragg's angle. Crystallite size was found to be about 12.3 nm from the most intensive peak of NPs XRD spectra.

3.4. Morphology and Elemental Analysis. Morphology of TiO_2 NPs and EPD film was investigated using SEM and is shown in Figure 2. TiO_2 NPs formed were spherical in shape and mostly of uniform size as can be seen from Figure 2(a). The surface morphological characterization highlighted the importance of NPs preparation in maintaining the nanostructured phase. The particle growth after the nucleation of primary particles was affected by the solvents used during the microwave irradiation due to their dielectric constant and led to spherical shaped particles as can be seen from SEM (Figure 2(a)). Figure 2(b) shows the SEM of TiO_2 EPD film. It is clear from the SEM that the films are uniformly deposited over the substrate surface. Some agglomeration is also observed in the SEM, which may be due to annealing

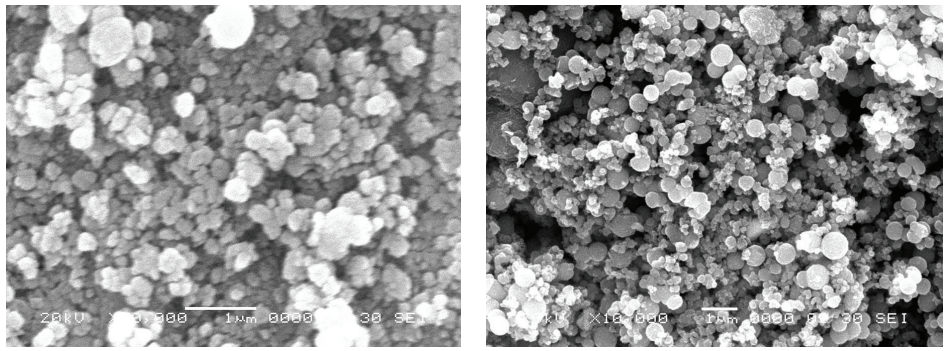

(a) (b)

Figure 2: SEM image of TiO_2 after air annealing at 500°C (a) NPs and (b) EPD TiO_2 film on steel substrate.

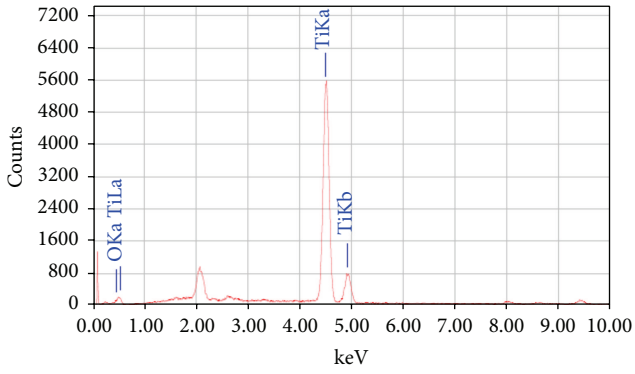

Figure 3: EDS spectra of TiO_2 NPs.

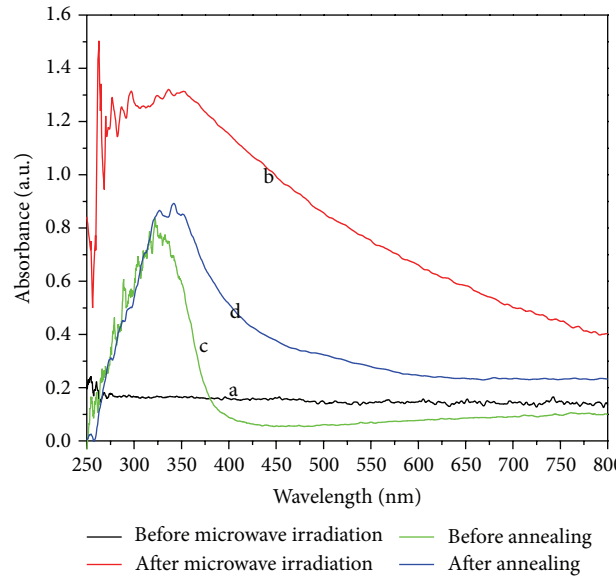

Figure 4: UV-Vis absorption spectra of (a) TiO_2 NP's before microwave irradiation, (b) TiO_2 NP's after microwave irradiation and air annealing at 500°C, (c) EPD TiO_2 thin film, and (d) EPD TiO_2 thin film after air annealing at 500°C.

of TiO_2. SEM shows the porous nature of film, suitable for absorption of dye through nanopores for improved catalytic activity.

Elemental analysis of TiO_2 NPs was done by using EDS and is shown in Figure 3. The peaks of the spectra show the presence of titanium and oxygen elements. Quantitative analysis indicated that the atomic composition of Ti and O is in stoichiometric ratio.

3.5. Absorption Analysis. The UV-Visible absorption spectrum of TiO_2 NPs, before and after microwave irradiation, and EPD TiO_2 film, as deposited and air annealed at 500°C, are shown in Figure 4. UV-Vis absorption spectra clearly indicate crystallization of TiO_2 after microwave irradiations and air annealing at 500°C showing absorption peak at around 345 nm wavelength which is blue shifted in comparison to bulk TiO_2. UV-Vis spectra of EPD thin film are also shown in the figures, that is, curves c and d. It is observed from the spectra that after air annealing absorbance peak of EPD film is red shifted which is due to increase in grain size.

3.6. BET Analysis. Surface area analysis was done by using BET surface analyzer; assuming NPs to be of spherical shape, particle size can be calculated from surface area values using following equation [28]:

$$d = \frac{6}{\rho S_{\mathrm{BET}}}, \tag{6}$$

where ρ is the density of TiO_2 particles (taken as 4.23 g/cm^3) and S_{BET} is the BET surface area. For powder sample heated at 500°C, the measured BET surface area has been found to be 43.52 m^2/g, giving particle size of 33 nm from above equation (6).

3.7. Photocatalytic (PC) Activity. Mechanism for PC degradation [29] of a dye can be explained as follows. UV-light illumination on the catalyst surface with enough energy leads to formation of a hole (h^+) in the valence band and an

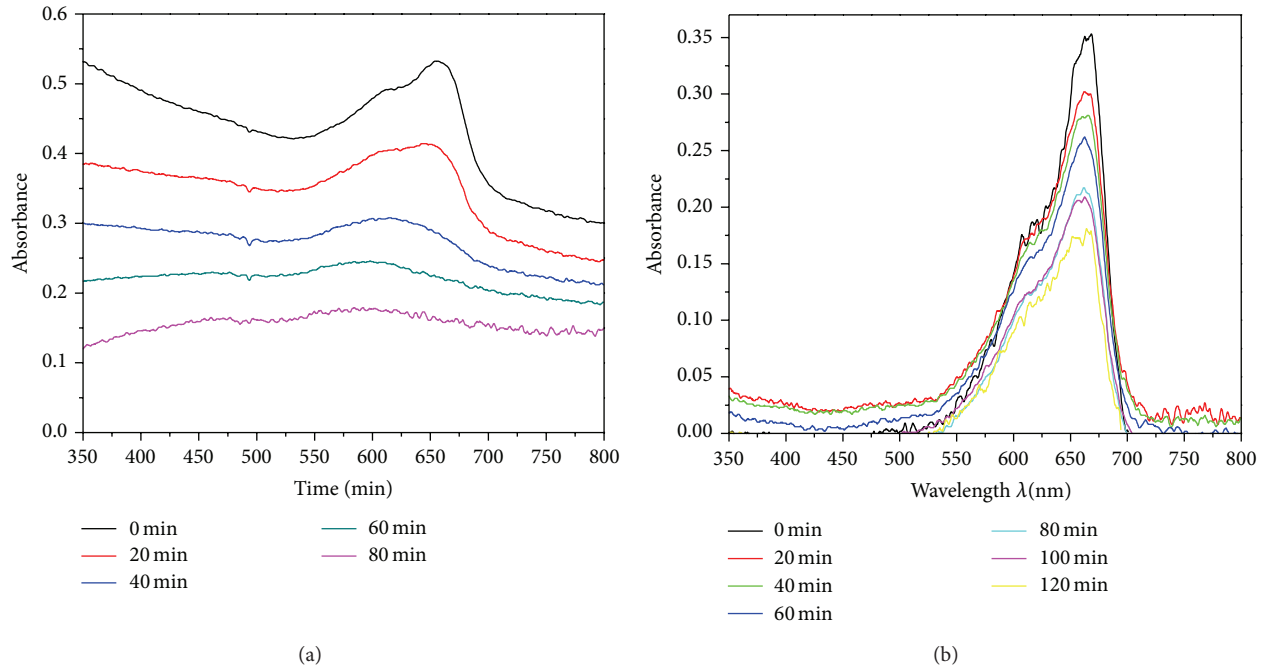

FIGURE 5: Photodegradation of MB under UV irradiations at different times using (a) TiO_2 NPs and (b) EPD TiO_2 film.

electron (e^-) in the conduction band. The hole oxidizes either pollutant directly or water to produce $OH^\bullet$ radicals, whereas the electron in the conduction band reduces the oxygen adsorbed on the catalyst. The activation of TiO_2 by UV light can be represented by the following steps:

$$TiO_2 + h\nu \longrightarrow e^- + h^+ \quad (7)$$

$$e^- + O_2 \longrightarrow O_2^- \quad (8)$$

In this reaction, h^+ and e^- are powerful oxidizing and reductive agents, respectively. The oxidative and reductive reaction steps are expressed as follows:

$$h^+ + MG \longrightarrow \text{degradation compounds} \quad (9)$$

$$h^+ + H_2O \longrightarrow OH^\bullet + H^+ \quad (10)$$

$$OH^- + MG \longrightarrow \text{degradation compounds} \quad (11)$$

Titanium dioxide (TiO_2) has both a high oxidation potential and a band gap that allows for absorption of the UV light. Both the reduction and oxidation sites are located on the TiO_2 surface, and the reduction of adsorbed oxygen molecules proceeds on the TiO_2 surface. Titanium dioxide forms highly oxidizing holes and photogenerated electrons resulting in powerful oxidizing and reductive agents hydroxyl radicals and superoxides.

The PC activities of synthesized TiO_2 NPs and EPD film were evaluated according to their photodegradation rates of MB dye, which is of high concentration, and MR dye, which is of low concentration in aqueous solution. The UV-Visible absorbance spectra of TiO_2 NPs and EPD TiO_2 film with UV light irradiation time for MB and MR dyes are shown in Figures 5 and 6, respectively. From the plot it is observed that with the increase in irradiation time, concentration of dyes decreases which is shown by decrease in absorbance. The percentage efficiency of photo degradation of dyes (also known as decolourising ratio) using TiO_2 NPs and film was determined using following equation [29]:

$$X = \frac{C_0 - C}{C_0} \times 100, \quad (12)$$

where C_0 and C are the solution concentration before and after degradation. Figure 7 shows the percentage efficiency of photo degradation of MB and MR dyes with irradiation time for TiO_2 NPs and film. We observed that photodegradation efficiency increases with increasing irradiation time. The time courses of the photocatalytic degradation of NPs and film are 60 min and 120 min to achieve 50% degradation of MB dye, whereas for MR dye film has shown better efficiency. It was found that at 10 min, degradation reached 50% with film and correspondingly 15% with NPs.

The apparent rate constant for degradation of dye was obtained by calculating the correlation between the length of time of visible-light irradiation and the decreasing ratio of dye, determined using following equation [30]:

$$\ln\left(\frac{C_0}{C}\right) = K_{app} \cdot t \quad (13)$$

The slope of this plot is the apparent rate constant for degradation of dye. The plot in (C_0/C) with irradiation time for MB and MR dyes is shown in Figure 8 and the apparent rate constant for degradation of MB is 1.378×10^{-2} and 0.558×10^{-2}, respectively, for TiO_2 NPs and thin film and for degradation of MR dye is 1.761×10^{-2} and 11.627×10^{-2},

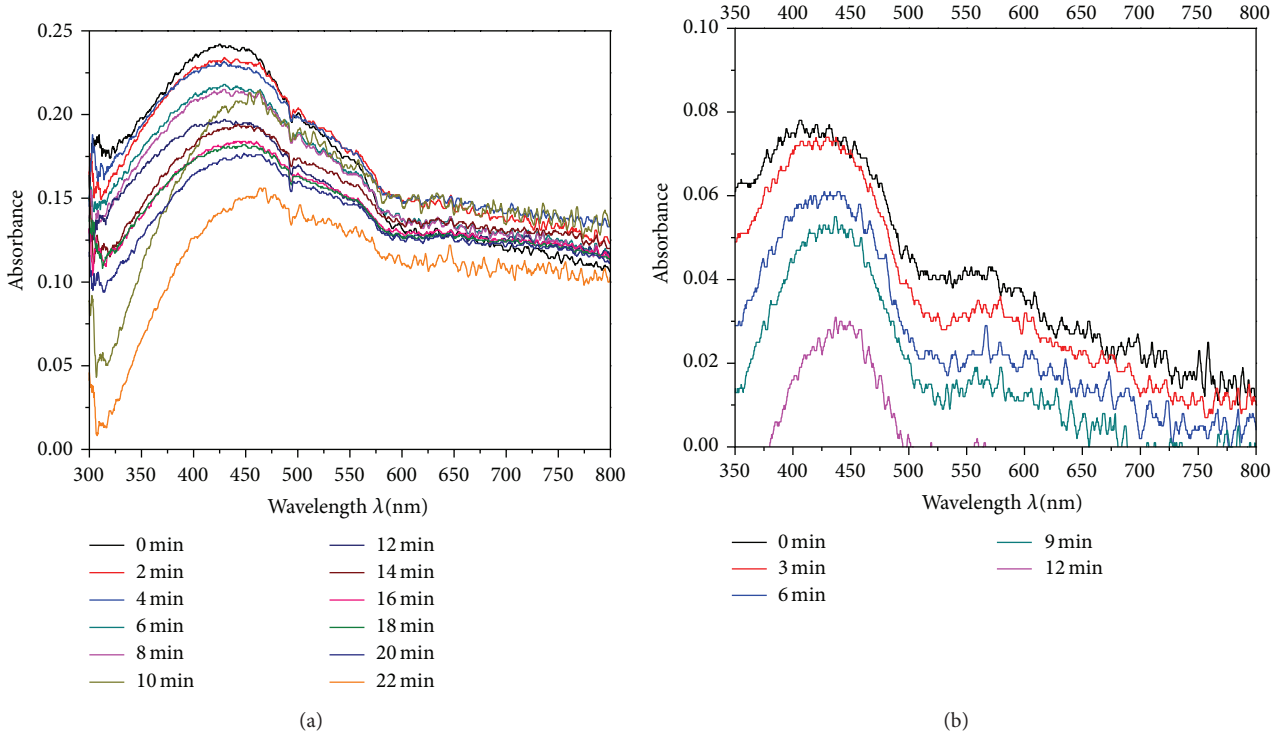

Figure 6: Photodegradation of MR under UV irradiations at different times using (a) TiO_2 NPs and (b) EPD TiO_2 film.

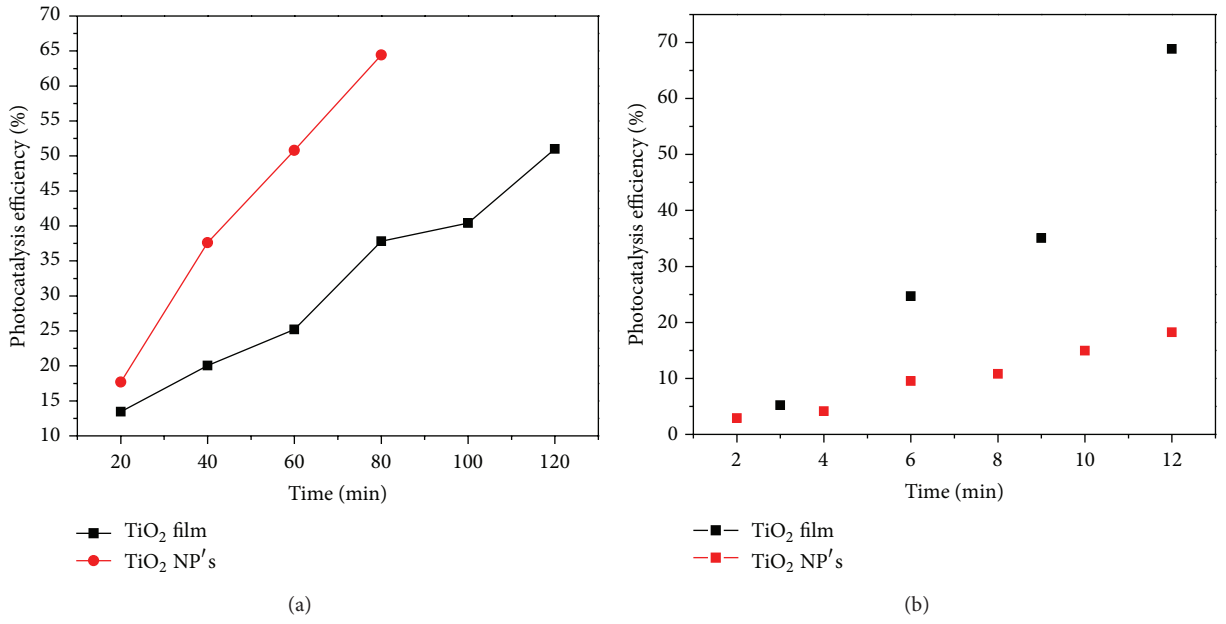

Figure 7: Efficiency of degradation of TiO_2 NPs and EPD TiO_2 film under UV light for (a) MB and (b) MR dyes.

respectively, for TiO_2 NPs and thin film. From Figures 5–8 it can be seen that efficiency and apparent rate constant (K_{app}) show almost linear relationship with the photodegradation of both MB and MR solutions and for MB dye this rate is high with TiO_2 NPs whereas for MR dye rate it is high with TiO_2 film (about an order higher in both cases). This shows that the PC rate varies with the form of TiO_2 as well as dye.

The PC properties of TiO_2 are also reported to depend on the reactivity of TiO_2 with water and its decomposition products, oxygen and hydrogen. These properties further depend on (a) effect of defect disorder on semiconducting properties, (b) effect of light on semiconductor properties, (c) effect of semiconductor properties on reactivity and PC of TiO_2 with water, and (d) the effect of light on the electrochemical

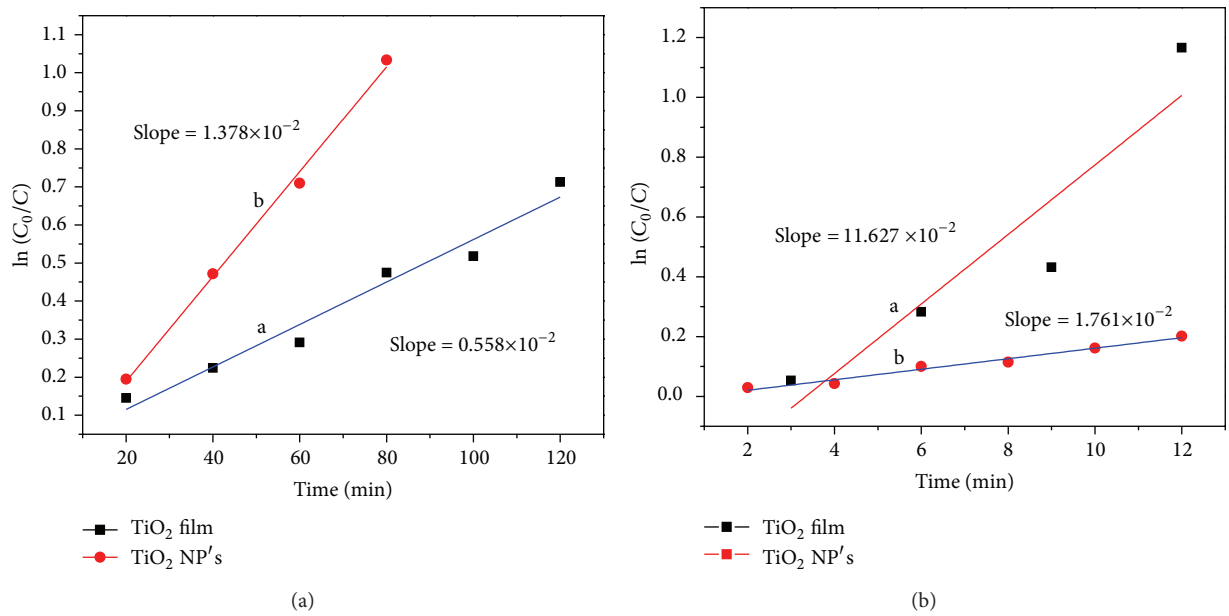

Figure 8: Apparent rate of degradation under UV light with TiO_2 Film and TiO_2 NP's for (a) MB and (b) MR dyes.

properties of the TiO_2/H_2O interface. Related concept has been outlined in the reference paper [31].

4. Conclusions

Highly active porous crystalline anatase TiO_2 NPs were prepared by using microwave assisted method and TiO_2 thin film using cathodic EPD on steel substrate in acidic electrolyte solution. High dielectric constant of solvent led to strong interaction with microwave radiations to form spherical aggregates of nanosized crystalline titania. Deposited NPs and film are highly porous and of uniform size and thickness. Annealed TiO_2 NPs and EPD TiO_2 thin film have shown excellent PC degradation property for MB and MR dyes. NPs show better efficiency for MB dye than EPD film (50% degradation using NPs in 60 minutes compared to 120 minutes using film) whereas EPD film has shown higher PC activity for MR dye. This study points the way to the commercialization of PC through thin film for reusability.

Conflict of Interests

The authors declare that there is no conflict of interests regarding the publication of this paper.

Acknowledgments

The authors are thankful to Director of ARDE, Pune, India, for granting permission to publish this work. Thanks are also due to HEMRL, Pune, for BET of samples and Physics Department University of Pune for XRD, SEM, and EDS of samples.

References

[1] K. Hashimoto, H. Irie, and A. Fujishima, "TiO_2 photocatalysis: a historical overview and future prospects," *Japanese Journal of Applied Physics, Part 1: Regular Papers and Short Notes and Review Papers*, vol. 44, no. 12, pp. 8269–8285, 2005.

[2] J. W. Kim, H. S. Kim, K. H. Yu, A. Fujishima, and Y. S. Kim, "Enhanced photocatalytic activity of 3,4,9,10-perylenetetracarboxylic diimide modified titanium dioxide under visible light irradiation," *Bulletin of the Korean Chemical Society*, vol. 31, no. 10, pp. 2849–2853, 2010.

[3] B. Tan and Y. Wu, "Dye-sensitized solar cells based on anatase TiO_2 nanoparticle/nanowire composites," *Journal of Physical Chemistry B*, vol. 110, no. 32, pp. 15932–15938, 2006.

[4] P. I. Gouma, M. J. Mills, and K. H. Sandhage, "Fabrication of free-standing titania-based gas sensors by the oxidation of metallic titanium foils," *Journal of the American Ceramic Society*, vol. 83, no. 4, pp. 1007–1009, 2000.

[5] J. A. Herrera Melian, J. M. Dona Rodriguez, A. V. Suarez et al., "The photocatalytic disinfection of urban wastewaters," *Chemosphere*, vol. 41, pp. 323–327, 2000.

[6] T. Sugimoto, X. Zhou, and A. Muramatsu, "Synthesis of uniform anatase TiO_2 nanoparticles by gel-sol method: 3. Formation process and size control," *Journal of Colloid and Interface Science*, vol. 259, no. 1, pp. 43–52, 2003.

[7] J. Tang, F. Redl, Y. Zhu, T. Siegrist, L. E. Brus, and M. L. Steigerwald, "An organometallic synthesis of TiO_2 nanoparticles," *Nano Letters*, vol. 5, no. 3, pp. 543–548, 2005.

[8] S. Jeon and P. V. Braun, "Hydrothermal synthesis of Er-doped luminescent TiO_2 nanoparticles," *Chemistry of Materials*, vol. 15, no. 6, pp. 1256–1263, 2003.

[9] D. Byun, Y. Jin, B. Kim, J. Kee Lee, and D. Park, "Photocatalytic TiO_2 deposition by chemical vapor deposition," *Journal of Hazardous Materials*, vol. 73, no. 2, pp. 199–206, 2000.

[10] M. O. Abou-Helal and W. T. Seeber, "Preparation of TiO_2 thin films by spray pyrolysis to be used as a photocatalyst," *Applied Surface Science*, vol. 195, no. 1–4, pp. 53–62, 2002.

[11] S. Takeda, S. Suzuki, H. Odaka, and H. Hosono, "Photocatalytic TiO_2 thin film deposited onto glass by DC magnetron sputtering," *Thin Solid Films*, vol. 392, no. 2, pp. 338–344, 2001.

[12] P. Periyat, N. Leyland, D. E. McCormack, J. Colreavy, D. Corr, and S. C. Pillai, "Rapid microwave synthesis of mesoporous TiO_2 for electrochromic displays," *Journal of Materials Chemistry*, vol. 20, no. 18, pp. 3650–3655, 2010.

[13] L. Pan, Z. Sun, and C. Q. Sun, "Nanocatalysts synthesized via microwave-assisted solution phase synthesis for efficient photocatalysis," *Journal of Materials Chemistry A*, vol. 1, pp. 8299–8326, 2013.

[14] J.-G. Yu, H.-G. Yu, B. Cheng, X.-J. Zhao, J. C. Yu, and W.-K. Ho, "The effect of calcination temperature on the surface microstructure and photocatalytic activity of TiO_2 thin films prepared by liquid phase deposition," *Journal of Physical Chemistry B*, vol. 107, no. 50, pp. 13871–13879, 2003.

[15] B. Neppolian, H. C. Choi, S. Sakthivel, B. Arabindoo, and V. Murugesan, "Solar/UV-induced photocatalytic degradation of three commercial textile dyes," *Journal of Hazardous Materials*, vol. 89, no. 2-3, pp. 303–317, 2002.

[16] W. Baran, A. Makowski, and W. Wardas, "The effect of UV radiation absorption of cationic and anionic dye solutions on their photocatalytic degradation in the presence TiO_2," *Dyes and Pigments*, vol. 76, no. 1, pp. 226–230, 2008.

[17] M. Zhou, J. Yu, S. Liu, P. Zhai, and L. Jiang, "Effects of calcination temperatures on photocatalytic activity of SnO_2/TiO_2 composite films prepared by an EPD method," *Journal of Hazardous Materials*, vol. 154, no. 1–3, pp. 1141–1148, 2008.

[18] I. Corni, M. P. Ryan, and A. R. Boccaccini, "Electrophoretic deposition: from traditional ceramics to nanotechnology," *Journal of the European Ceramic Society*, vol. 28, no. 7, pp. 1353–1367, 2008.

[19] U. G. Akpan and B. H. Hameed, "Parameters affecting the photocatalytic degradation of dyes using TiO_2-based photocatalysts: a review," *Journal of Hazardous Materials*, vol. 170, no. 2-3, pp. 520–529, 2009.

[20] D. S. Kim and S.-Y. Kwak, "The hydrothermal synthesis of mesoporous TiO_2 with high crystallinity, thermal stability, large surface area, and enhanced photocatalytic activity," *Applied Catalysis A: General*, vol. 323, pp. 110–118, 2007.

[21] J. Zhang, X. Xiao, and J. Nan, "Hydrothermal-hydrolysis synthesis and photocatalytic properties of nano-TiO_2 with an adjustable crystalline structure," *Journal of Hazardous Materials*, vol. 176, no. 1–3, pp. 617–622, 2010.

[22] M. Song, L. Bian, T. Zhou, and X. Zhao, "Surface ζ potential and photocatalytic activity of rare earths doped TiO_2," *Journal of Rare Earths*, vol. 26, no. 5, pp. 693–699, 2008.

[23] I. K. Konstantinou and T. A. Albanis, "TiO_2-assisted photocatalytic degradation of azo dyes in aqueous solution: kinetic and mechanistic investigations: a review," *Applied Catalysis B: Environmental*, vol. 49, no. 1, pp. 1–14, 2004.

[24] D. Jiang, H. Zhao, S. Zhang, and R. John, "Kinetic study of photocatalytic oxidation of adsorbed carboxylic acids at TiO_2 porous films by photoelectrolysis," *Journal of Catalysis*, vol. 223, no. 1, pp. 212–220, 2004.

[25] J. Li, L. Zheng, L. Li, Y. Xian, and L. Jin, "Fabrication of TiO_2/Ti electrode by laser-assisted anodic oxidation and its application on photoelectrocatalytic degradation of methylene blue," *Journal of Hazardous Materials*, vol. 139, no. 1, pp. 72–78, 2007.

[26] N. Koura, T. Tsukamoto, H. Shoji, and T. Hotta, "Preparation of various oxide films by an electrophoretic deposition method: a study of the mechanism," *Japanese Journal of Applied Physics, Part 1: Regular Papers & Short Notes & Review Papers*, vol. 34, no. 3, pp. 1643–1647, 1995.

[27] P. B. Bagdare, S. B. Patil, and A. K. Singh, "Phase evolution and PEC performance of $Zn_xCd_{(1-x)}S$ nanocrystalline thin films deposited by CBD," *Journal of Alloys and Compounds*, vol. 506, no. 1, pp. 120–124, 2010.

[28] J. Wang, J. Polleux, J. Lim, and B. Dunn, "Pseudocapacitive contributions to electrochemical energy storage in TiO_2 (anatase) nanoparticles," *Journal of Physical Chemistry C*, vol. 111, no. 40, pp. 14925–14931, 2007.

[29] A. K. Singh and U. T. Nakate, "Photocatalytic properties ofmicrowave-synthesized TiO_2 and ZnO nanoparticles using malachite green dye," *Journal Nanoparticles*, vol. 2013, Article ID 310809, 7 pages, 2013.

[30] S. Ghasemi, S. Rahimnejad, S. Rahman Setayesh, S. Rohani, and M. R. Gholami, "Transition metal ions effect on the properties and photocatalytic activity of nanocrystalline TiO_2 prepared in an ionic liquid," *Journal of Hazardous Materials*, vol. 172, no. 2-3, pp. 1573–1578, 2009.

[31] T. Bak, J. Nowotny, N. J. Sucher, and E. D. Wachsman, "Photocatalytic water disinfection on oxide semiconductors: part 1—basic concepts of TiO_2 photocatalysis," *Advances in Applied Ceramics*, vol. 111, no. 1-2, pp. 4–15, 2012.